Ultrasound combined with contrast-enhanced ultrasound in the diagnosis of primary squamous cell carcinoma of the thyroid: A case report and literature review

CUIE CHEN[1*], QIUXIAO XU[2*], YIJING DENG[2], JIANLING PENG[1], XUELING HE[2] and LIJUAN LIU[2]

[1]Department of Ultrasound, First Clinical Medical College, Guangdong Medical University, Zhanjiang, Guangdong 524002, P.R. China; [2]Department of Ultrasound, Affiliated Hospital of Guangdong Medical University, Zhanjiang, Guangdong 524002, P.R. China

Received September 19, 2024; Accepted December 4, 2024

DOI: 10.3892/ol.2025.14877

Abstract. Primary squamous cell carcinoma of the thyroid (PSCCT) is a rare malignancy with a poor prognosis. Therefore, early diagnosis and treatment are critical to the survival of patients and to improve their quality of life. However, diagnosing this illness is challenging. The present study describes the ultrasound (US) and contrast-enhanced US (CEUS) findings of PSCCT diagnosed in a 69-year-old woman with a rapidly enlarging neck mass. A total thyroidectomy was performed, and the results of postoperative pathology and immunohistochemical tests confirmed the diagnosis of PSCCT. Any other potential primary tumor site was excluded. This case and literature review provide a reliable reference for the diagnosis of PSCCT using US combined with CEUS. Radiologists should increase their understanding of this disease to achieve an early and accurate diagnosis.

Introduction

Primary squamous cell carcinoma of the thyroid (PSCCT) is a progressive and highly invasive tumor, accounting for ~0.1% of all primary thyroid malignancies (1). The origin of PSCCT is unclear, as the squamous epithelium is usually absent from the thyroid gland under normal physiological conditions. Currently, three theories have been proposed to explain the origin of PSCCT. First, PSCCT is hypothesized to originate from a residual branchial arch or thyroglossal ducts of embryonic origin (2). Second, underlying diseases such as Hashimoto's thyroiditis and inflammatory reactions trigger squamous metaplasia (3). Third, dedifferentiation of pre-existing primary thyroid cancers, such as medullary, papillary or anaplastic carcinomas, may cause PSCCT (4). The World Health Organization (WHO) reclassified PSCCT as a subtype of anaplastic carcinoma rather than a separate entity in 2022 (5).

Patients with PSCCT are frequently diagnosed at an advanced stage. An early stage diagnosis is challenging due to the rare occurrence of this malignancy and the absence of typical imaging manifestations. The current study presents a case of PSCCT and describes the process of its diagnosis based on findings from ultrasound (US) combined with contrast-enhanced US (CEUS). To the best of our knowledge, the present case study is the most thoroughly documented profile among the six instances of PSCCT recorded in the history of the Affiliated Hospital of Guangdong Medical University (Zhanjiang, China). In addition, the available literature on PSCCT diagnosis and treatment is summarized.

Case report

Patient. A 69-year-old woman presented at the Affiliated Hospital of Guangdong Medical University in October 2022 with a painless right-sided neck mass that had been rapidly enlarging for the last 2 months (Fig. 1). In addition, the patient had lost 13 kg of weight within this short duration. As the disease progressed, local ulceration of the skin was observed on the right side of the neck, with yellowish ooze and hyperpigmentation. At 5 months prior to this presentation, the patient had been diagnosed with poorly differentiated adenocarcinoma of the stomach and underwent a laparoscopic distal gastrectomy for gastric cancer (Billroth II procedure). The patient did not have any family history of thyroid cancer or any other type of cancer, nor had neck radiation ever been administered.

Two heterogeneous echogenic masses in the right lobe of the thyroid gland were visible on thyroid US in October 2022. Lesion A, a mixed cystic-solid mass measuring 5.7x4.3x5.6 cm,

Correspondence to: Dr Lijuan Liu, Department of Ultrasound, Affiliated Hospital of Guangdong Medical University, 57 Renmin Avenue South, Xiashan, Zhanjiang, Guangdong 524002, P.R. China
E-mail: nmyl0901@163.com

*Contributed equally

Abbreviations: PSCCT, primary squamous cell carcinoma of the thyroid; WHO, World Health Organization; US, ultrasound; CEUS, contrast-enhanced ultrasound; CDFI, color Doppler flow imaging; RI, resistive index; ACR-TIRADS, American College of Radiology-Thyroid Imaging and Reporting Data System; SSCCT, secondary SCCT

Key words: primary SCC, thyroid cancer, US, CEUS, diagnosis

was situated in the lower middle region of the right lobe of the thyroid gland (Fig. 2A). The lower edge extended beyond the superior sternal fossa. Lesion B was a solid, slightly hyperechoic nodule measuring 2.6x1.7x2.3 cm, occupying the upper part of the ipsilateral lobe (Fig. 3A). These lesions showed some of the malignant ultrasonic characterizations, such as irregular margins and unclear boundaries with adjacent soft-tissue layers. In addition, two irregular macrocalcifications and microcalcifications were observed in Lesion A. Color Doppler flow imaging (CDFI) displayed abundant blood flow signals inside the lesion (Fig. 2B), with a resistive index (RI) of 0.80 in one of the arteries (Fig. 2C). Lesion B showed an abundant blood flow signal in and around the nodule on CDFI (Fig. 3B). CEUS was performed after injecting 2.0 ml SonoVue® (Bracco).

Lesion A presented as an inhomogeneous hypo-enhanced thyroid nodule with a broad central area of non-enhancement and blurred borders (Fig. 2D). Lesion B, observed in reperfusion mode, had unclear boundaries with abundant contrast agent inside the lesion. Based upon the conventional malignant findings in US and CEUS patterns, these two nodules merited 10 points (mixed cystic-solid, 1 point; hypoechoic, 2 points; irregular margins and unclear boundaries with adjacent soft-tissue layers, 3 points; macrocalcifications, 1 point; and microcalcifications, 3 points) and were evaluated as category 5 in the 2017 American College of Radiology-Thyroid Imaging and Reporting Data System (ACR-TIRADS) (6). Therefore, these nodules were preliminarily diagnosed as malignant tumors.

Following these findings, the clinician performed a coarse-needle biopsy of the thyroid mass, which showed an SCCT. Immunohistochemical findings were positive for cytokeratin (CK)19, CK5/6, p63, p53, Ki67 and paired box protein Pax-8 (PAX-8), and negative for thyroid peroxidase and thyroid transcription factor 1 (TTF-1). A diagnosis of PSCCT was eventually established only after excluding all other possible primary tumor sites. Considering the large size of the tumor and the fact that the patient was in the postoperative period of gastric cancer, the patient was started on palliative treatment with oral anlotinib (12 mg daily on days 1-14), intravenous paclitaxel (200 mg on day 1 every 3 weeks) and intravenous tislelizumab (300 mg on day 1 every 3 weeks) (for two cycles lasting 21 days).

The patient underwent another US and CEUS examination after the second cycle of palliative treatment in December 2022. Lesion A was smaller (3.5x2.6x3.3 cm) than its initial size, and the RI (0.65) was decreased compared with its initial value (Fig. 4A-C). CEUS still showed heterogeneous hypo-enhancement of the nodule with blurred boundaries, but the percentage of internal non-enhancing areas was higher than the initial percentage (Fig. 4D). The boundary of Lesion B became clearer with a uniform and continuous hyperechoic thin halo visible around it, and there was no marked change in its size (Fig. 5A). CDFI showed an increase in the internal blood flow signal of the nodule, and the periphery appeared to have a circumferential blood flow signal (Fig. 5B). Correspondingly, CEUS showed a uniformly high enhancement of the nodule with a clearer boundary (Fig. 5C). Finally, the original diagnosis of Lesion A was maintained and the risk classification of Lesion B was downgraded from category 5 to category 3 in ACR-TIRADS.

Subsequently, the patient underwent a total thyroidectomy with right modified radical neck dissection and bilateral central node dissection. Postoperative pathology revealed Lesion A as an SCCT, with mostly coagulative necrosis, and Lesion B as nodular goiter, with adenomatous nodule formation (Fig. 6). In addition, none of the lymph nodes were metastatic, and cancerous invasion of the left thyroid gland had not occurred. Adjuvant radiotherapy was suggested to the patient and their family, but was refused. Finally, tislelizumab (200 mg in day 1 of each cycle, every 3 weeks) was administered as maintenance immunotherapy. Follow-up was performed every 3 months, and the patient is currently alive with no tumor recurrence after 19 months of surgery.

Immunohistochemistry. Tissues were fixed in 10% neutral formalin fixative immediately after sampling. For fixation, 10% neutral formalin (neutral buffered formalin) was used at room temperature, for 24 h. Conventional paraffin was used for embedding. The section thickness was 3-5 μm, using standard paraffin sectioning methods. In order to fully expose the antigen, thermal repair with 0.01 M citrate buffer (pH 6.0) was performed, heating the sections at 95-100˚C for 10-20 min in a microwave or water bath. Primary antibodies (dilution, 1:100 to 1:500; all Abcam) were incubated with the sections overnight at 4˚C. An HRP-conjugated secondary antibody (dilution, 1:200 to 1:1,000; Dako; Agilent Technologies, Inc.) was added and incubated at room temperature for 30-60 min. 3,3'-diaminobenzidine was applied for 3-10 min as the chromogenic substrate. Contrast staining was performed using hematoxylin for 1-3 min, followed by dehydration and sealing. Observation was carried out using a light microscope.

Pathology. Post-operative pathology tissues were fixed using 10% neutral formalin at room temperature for 24 h, followed by paraffin embedding. Tissues were sections at 3-5 μm using a standard microtome. Hematoxylin and eosin staining was performed to observe histological features. Hematoxylin was applied at room temperature for 5 min, and eosin staining was performed at room temperature for 2 min. This was followed by dehydration, visualization and sealing. A light microscope was used to observe the sections.

Discussion

PSCCT is a rare and highly aggressive thyroid malignancy with a short median survival time that accounts for ~0.1% of all primary thyroid cancer cases (1). Notably, older individuals aged 50 to 60 years are typically affected, and the ratio of women to men is 2.5:1.7 (7). PSCCT manifests as a fast growing tumor in the anterior neck. Dysphagia, vocal abnormalities and dyspnea are additional typical symptoms (8). An early diagnosis increases the probability of timely treatment, prolongs the duration of patient survival and improves the quality of life for patients. Therefore, clinical studies should focus on finding improved methods to determine an early diagnosis.

The preferred imaging technique for thyroid nodule diagnosis is US. Several ultrasonic characteristics, including solid components, microcalcifications, hypoechogenicity, taller-than-wide dimensions and irregular margins, indicate

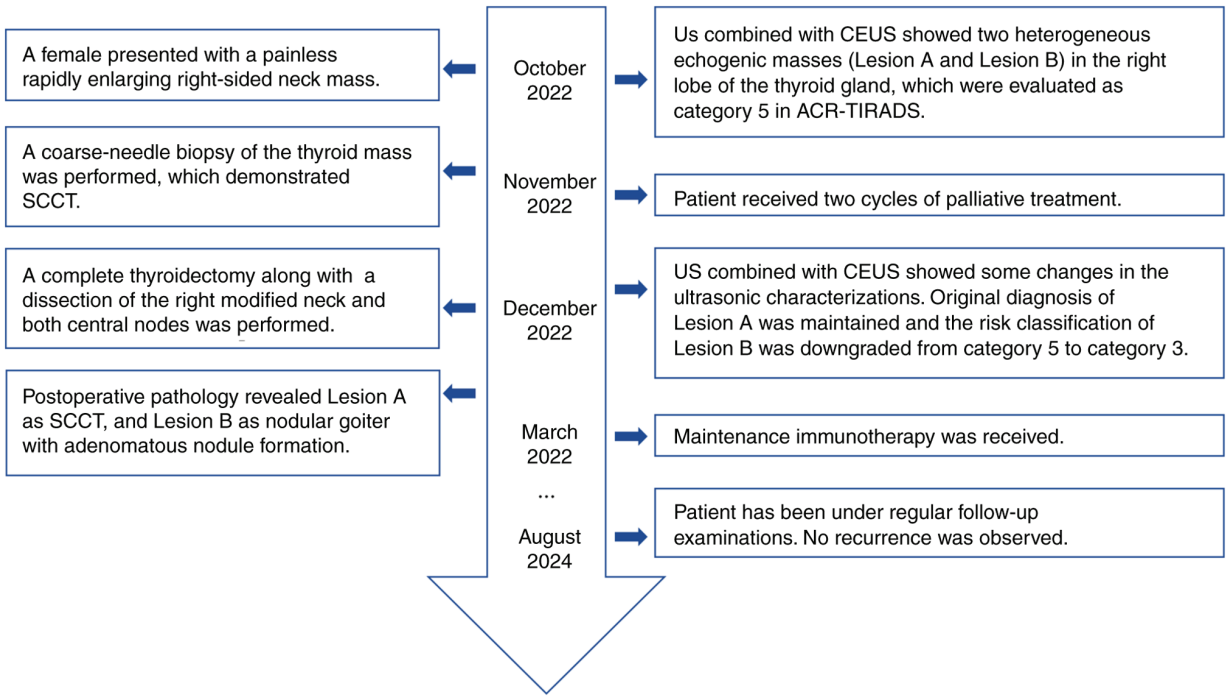

Figure 1. A timeline of the patient's diagnosis and treatment process. US, ultrasound; CEUS, contrast-enhanced US; ACR-TIRADS, American College of Radiology-Thyroid Imaging and Reporting Data System; SSCCT, secondary squamous cell carcinoma of the thyroid.

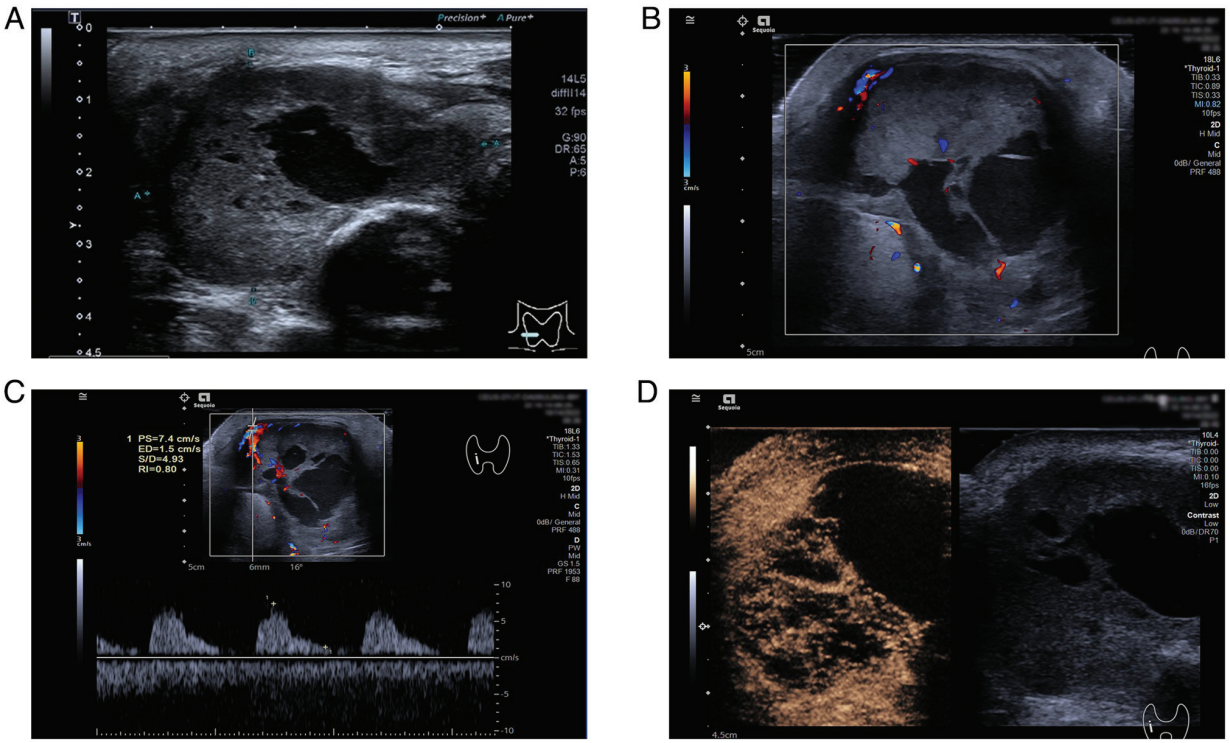

Figure 2. Combined US and CEUS findings of Lesion A before treatment. (A) US showed a mixed cystic-solid mass with irregular margins, macrocalcifications and microcalcifications inside. (B) Color Doppler flow imaging showed abundant blood flow signals inside. (C) One of the arteries demonstrated a PS of 7.4 cm/sec, an ED of 1.5 cm/sec, a S/D of 4.9 and an RI of 0.80. (D) CEUS showed an inhomogeneous hypo-enhanced thyroid nodule with a broad central area of non-enhancement and unclear boundaries. US, ultrasound; CEUS, contrast-enhanced US; RI, resistive index; PS, peak systolic velocity; ED, end diastolic velocity; S/D, systolic-to-diastolic ratio.

thyroid malignancy. Nevertheless, the ultrasonic features of PSCCT are not yet fully understood due to the limited number of reported cases. Yan *et al* (7) reported that ~85.7% (6/7) of PSCCTs on US were hypoechoic or mixed echoes with heterogeneous echogenicity, that 57.1% (4/7) revealed calcification and that all nodules had blood flow signals within

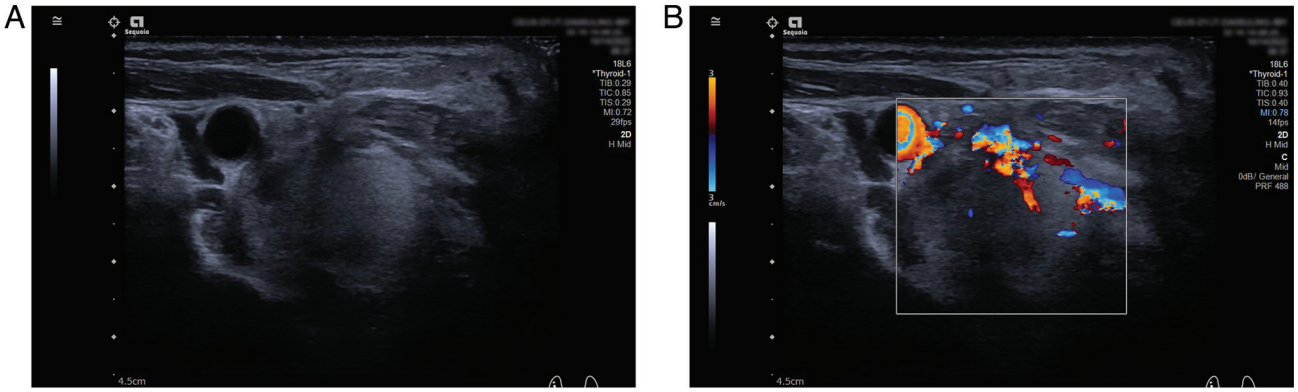

Figure 3. US and color Doppler findings of Lesion B before treatment. (A) US showed a solid slightly hyperechoic nodule with unclear boundaries. (B) Color Doppler flow imaging showed abundant blood flow signals in and around the nodule. US, ultrasound; CEUS, contrast-enhanced US; RI, resistive index; TIS, thermal index for soft tissue; TIB, thermal index for bone; TIC, thermal index for cranial bone; MI, mechanical index.

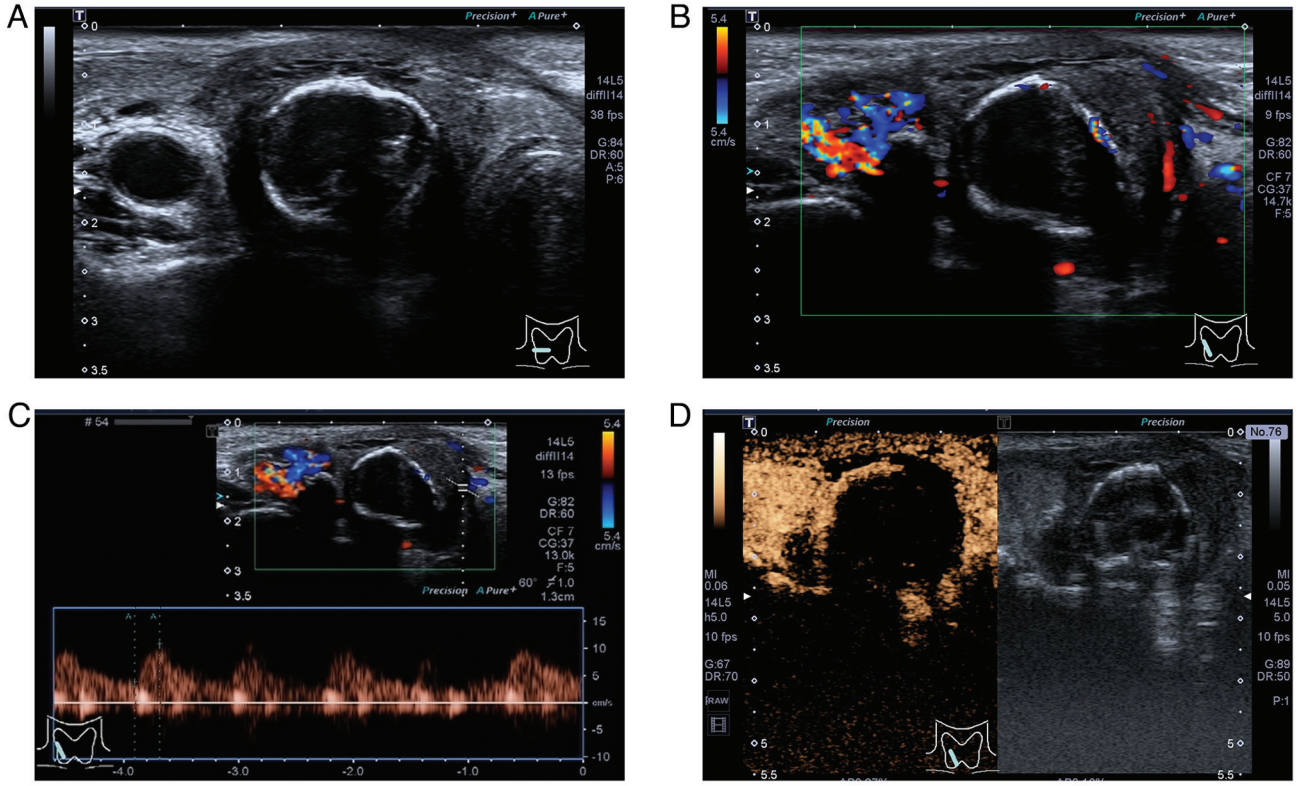

Figure 4. Combined US and CEUS findings of Lesion A after treatment. (A) US revealed that the size had significantly reduced. (B) Color Doppler flow imaging showed abundant blood flow signals inside. (C) The resistive index value was decreased to 0.65. (D) CEUS findings revealed that the percentage of non-enhancing areas within the nodule was higher than the percentage before treatment. US, ultrasound; CEUS, contrast-enhanced US.

them. Zhang *et al* (9) observed the ultrasonic features of nine PSCCT tumors and concluded that PSCCTs tended to appear as solid nodules that were relatively large, hypoechoic or very hypoechoic, with intranodular vascularity and extrathyroidal extension. Ou *et al* (10) reported that ultrasonography characteristics of PSCCT were predominantly the presence of hypoechoic, hard, solid nodules with rough boundaries and a grade 1-2 blood flow signal, occasionally accompanied by necrosis and calcification. In the present case, PSCCT, i.e., Lesion A, manifested as a mixed cystic and solid thyroid nodule with irregular margins and indistinct borders with adjacent soft-tissue layers. In addition, macrocalcifications and microcalcifications were observed inside the tumor, and CDFI showed abundant vascular signals with a high RI. These malignant US findings were consistent with those reported in other national and international studies (7-10).

The PSCCT lesion measured ~5.7x4.3x5.6 cm before treatment; this size was comparatively greater than the mean size of thyroid tumors (2.2±1.9 cm) (11). This may be attributed to the quick proliferation of tumor cells and the aggressive nature of this malignancy. The irregular margins and unclear boundaries indicated possible invasion of adjacent tissue by the nodule. Irregular macrocalcifications and microcalcifications are also highly suspicious ultrasonic indicators for

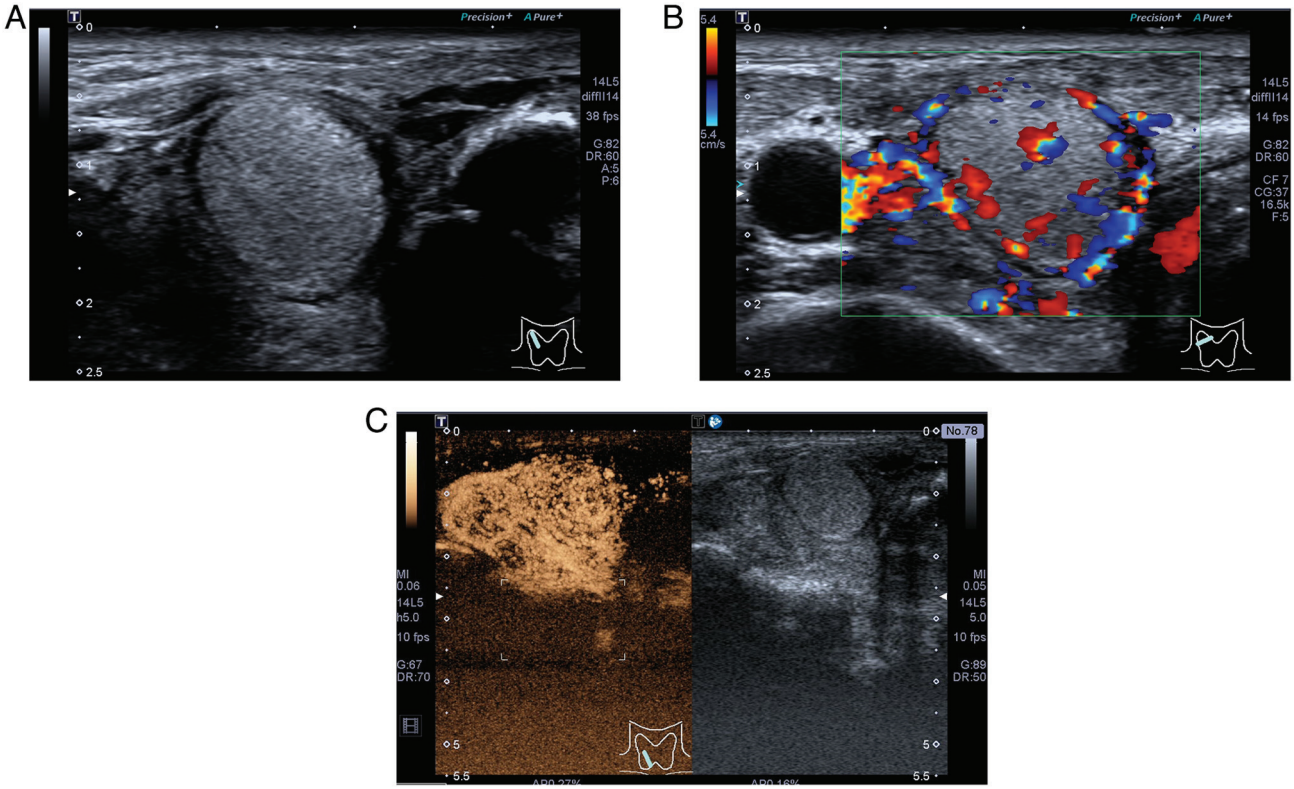

Figure 5. Combined US and CEUS findings of Lesion B after treatment. (A) US revealed that the boundary was clearer, and a uniform and continuous hyperechoic thin halo was present in the periphery. (B) Color Doppler flow imaging showed an increase in the internal blood flow signal of the nodule, and the periphery appeared to have a circumferential blood flow signal. (C) CEUS showed a uniformly high enhancement of the nodule with clearer boundaries. US, ultrasound; CEUS, contrast-enhanced US.

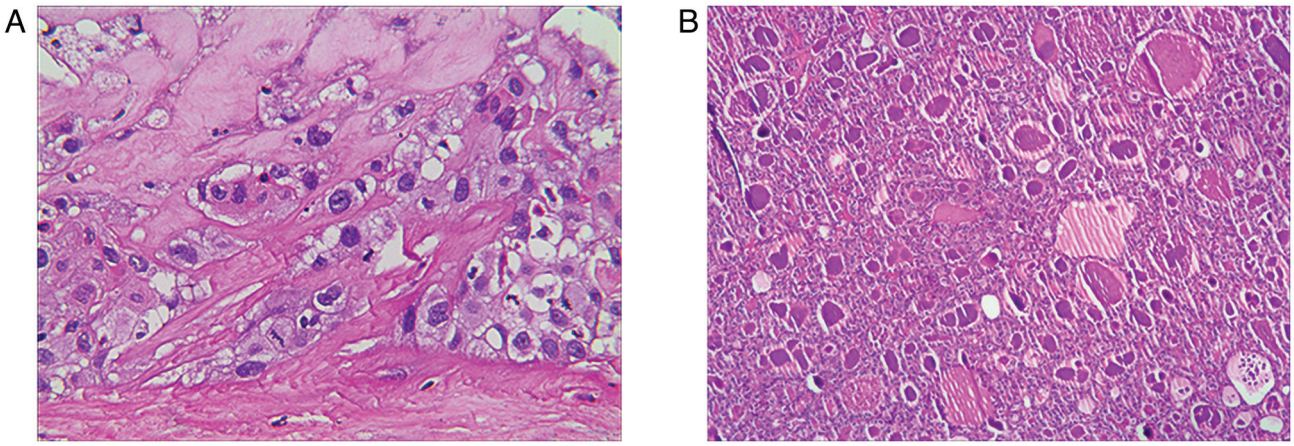

Figure 6. Pathological findings. (A) Hematoxylin and eosin staining of Lesion A (original magnification, x200). (B) Hematoxylin and eosin staining of Lesion B (original magnification, x100).

thyroid malignancy. Zhang *et al* (9) reported that the mean RI of PSCCTs was 0.84; this value was greater than the RIs of benign thyroid nodules (0.59) and papillary thyroid carcinomas (0.70). Approximately 87.5% of the available RIs were >0.70. The RI values reflect the blood flow resistance of arteries. The newly generated vascular networks may be prevented from maturing and pruning, as pro-angiogenic signaling is present continuously within the tumors. This results in poor vascular organization and malformations. Furthermore, elevated interstitial fluid pressure is a result of the high permeability of the tumor vasculature (12). Vascular structural malformations and tumor vascular compression may increase arterial resistance, which may be reflected in the RI value. In the present patient, intranodal vessels were observed on pre-treatment US with an RI of 0.80. This feature may reflect the aberrant neovascularization in the PSCCT.

The human thyroid gland has a rich blood supply; therefore, CEUS can be potentially useful in identifying and diagnosing benign and malignant thyroid nodules. However, limited reports are available on the CEUS imaging of PSCCT. Zhan and Ding (13)

reported on the CEUS presentation of thyroid nodules. It was found that the majority of malignant nodules showed slow inhomogeneous hypo-enhancement, whereas benign nodules showed rapid homogeneous overall hyper-enhancement, iso-enhancement or peripheral circumferential enhancement. Chen *et al* (14) indicated that CEUS displayed sustained low-peak enhancement of the PSCCT nodule, extending from its periphery to its center. In the current study, PSCCT presented as an inhomogeneous hypo-enhanced thyroid nodule with blurred borders and a broad central area of non-enhancement. This observation is similar to that reported by Chen *et al* (14) and consistent with the typical CEUS features of most malignant thyroid nodules. PSCCT may show uneven low enhancement due to several reasons, including the messy and irregular neovascularization of the malignant nodule and the uneven distribution of blood vessels. In addition, the infiltrative growth of the malignant nodule destroys the normal thyroid tissue and neovascularization in the surrounding area, which causes changes in the perfusion of the nodule, and makes it difficult for the contrast agent to enter into the inner part of the nodule. Rapid growth of tumor tissue can lead to an insufficient blood supply, resulting in necrosis and defects at the lesion site (15). In the present study, CEUS showed a large central area of nodules without enhancement, which was also consistent with the pathological changes of SCC and necrotic lesions. Notably, pathological necrosis is not always visible as anechoic/cystic areas on two-dimensional US sonograms but may also appear as solid inhomogeneous hypoechoic areas (16). In the present study, it was observed that ~97% of Lesion A showed coagulative necrosis with focal calcification and only a small amount of localized residual tumor tissue, whereas the percentage of anechoic/cystic areas and calcifications was <97% on US.

A solid nodule with decreased echogenicity is considered suspicious for malignancy (17). Unexpectedly, in the present study, Lesion B presented as a hypoechoic nodule but showed some of the malignant ultrasonic features, such as solid components, irregular margins and poor demarcation from adjacent soft-tissue layers, on the pre-treatment US. In a retrospective study, Liu *et al* (18) mentioned that some PSCCTs could appear as scattered hyperechoic nodules with a blood flow signal. Therefore, Lesion B was considered to be a malignant nodule. However, the size of Lesion B did not change markedly after two courses of treatment, indicating that it was not sensitive to antitumor drugs. By contrast, the boundaries of Lesion B became clearer than before, and a uniform and continuous hyperechoic thin halo appeared in the periphery. A homogeneous continuous hyperechoic thin halo of solid nodules is an important feature of benign nodules (19). Correspondingly, Lesion B presented as a homogeneous hyper-enhancement with well-defined borders on CEUS, indicating a benign lesion. The US and CEUS findings before and after antitumor therapy were compared, and the risk classification of Lesion B was finally downgraded from category 5 to category 3 based on the observations. Postoperative pathology showed that Lesion B was a nodular goiter with adenomatous nodule formation, validating the decision to adjust the grading.

Lesion B was misdiagnosed as a malignant nodule on initial US due to several reasons. First, Lesion A was considerably larger than Lesion B, and both lesions were adjacent to each other. Therefore, Lesion B could not be clearly distinguished from Lesion A, and they were tentatively considered of the same type. Additionally, a small percentage of malignant thyroid nodules are aggressive with rapid growth, and the internal blood supply may be hyper-enhanced on CEUS. Currently, typical CEUS imaging findings are not available due to the rarity of PSCCT, and a hyper-enhanced contrast pattern may be one of its imaging manifestations. It was impossible to exclude the possibility of a malignant lesion based on a hyper-enhanced contrast pattern.

Although imaging examinations have certain diagnostic value for PSCCT, the gold standard for its diagnosis is still a postoperative pathological tissue biopsy. Furthermore, immunohistochemistry is an effective technique for accurately diagnosing PSCCT and differentiating it from other metastatic SCCTs at different primary locations. Several PSCCT investigations revealed that TTF-1 is frequently positive in thyroid-originating cancers, such as papillary and follicular thyroid carcinomas, but rarely positive in PSCCT (20-22). CK7 and CK19 are diffusely expressed in PSCCT tissues, whereas CK20 is not expressed (23). PAX-8 is a significant biomarker of PSCCT. PAX-8 positivity usually indicates a PSCCT, whereas a negative result in a thyroid tumor generally indicates a metastatic SCC from another site (24). In the present case, the postoperative pathology revealed typical squamous cell morphology without any indication of additional thyroid cancer cells. In addition, the expression of the aforementioned immunohistochemical indicators supported the diagnosis of PSCCT. Notably, the patient had a history of gastric cancer, and the possibility of metastasis needed to be excluded for the accurate diagnosis of this thyroid mass.

Limited information is available on the molecular genetics of PSCCT. BRAF is a serine/threonine-specific protein kinase responsible for regulating cell division and survival (25). In a multi-institutional study, BRAFV600E mutations were found in 87.5% of PSCCT cases irrespective of thyroid differentiation status, and the prognosis of PSCCT was similar to that of anaplastic thyroid carcinoma (26). This supports the 2022 WHO classification of PSCCT as a subtype of anaplastic carcinoma (5). However, Ye *et al* (27) performed whole-exome sequencing of 15 PSCCT tissue samples from 15 different patients and reported the absence of BRAF mutations in these samples. Therefore, more research is required to understand the molecular genetics of PSCCT.

SCCT comprises PSCCT and secondary SCCT (SSCCT; metastasis or adjacent invasion), and their identification is a major challenge. PSCCT, the rarer form, typically affects one or both lobes of the thyroid gland, whereas SSCCT is usually multifocal (28). In the present case, PSCCT involved the right lobe of the thyroid gland, and the left lobe and isthmus were not involved, consistent with the findings of Ding *et al* (28). The ultrasonography characteristics of SCCT include a solid or nearly solid composition, hypoechoic and very hypoechoic echogenicity, irregular/lobulated margins, microcalcification and particularly extra-thyroidal invasion (16). PSCCT and SSCCT have similar clinicopathological and highly suspicious malignant ultrasonic features; therefore, it is difficult to differentiate them on thyroid imaging alone. One of the guidelines recommended for distinguishing SSCCT from PSCCT is to locate the primary tumor. Diagnostic tests, such as computed tomography, endoscopy and immunohistochemistry, can help to exclude SSCCT originating from the head and neck,

chest, upper gastrointestinal tract and pelvis (28). Overall, the findings of US or CEUS cannot be used to identify the pathological type of thyroid cancer. However, the possibility of PSCCT should be considered if certain ultrasonic features are observed. These features include a large mass that is solid or has both solid and cystic parts, appears hypoechoic on the scan, has irregular edges, contains internal microcalcifications, particularly extends beyond the thyroid, and shows uneven enhancement with blurred borders on CEUS.

The treatment of PSCCT is not standardized due to the lack of sufficient research evidence. Surgery can increase survival times by lowering tumor load and local invasion, and has been recognized as the treatment of choice. The median overall survival time of patients with complete macroscopic resection is increased by ~7 months compared with that of patients who undergo incomplete macroscopic resection (29). However, whether adjuvant chemoradiation benefits patients with PSCCT is still controversial. A population-based study summarized that extensive surgical treatments combined with adjuvant radiotherapy showed the best prognosis compared with surgery alone, radiotherapy alone, and no surgery and radiotherapy, with a median survival time of 11 months (1). Ou *et al* (10) indicated that the addition of radiotherapy and chemotherapy to surgical treatment may partially stop the growth of PSCCT. However, Au *et al* (30) demonstrated that neither adjuvant radiotherapy nor chemotherapy was associated with the survival prognosis in patients with PSCCT. In the present case, re-examination of the US after the second cycle of palliative treatment showed a significant reduction in the size of Lesion A and a decrease in the RI. CEUS findings revealed that the percentage of non-enhancing areas within the nodule after treatment was higher than the percentage before treatment. These sonographic changes indicated that the treatment was effective. This may be related to the benefit of preoperative neoadjuvant chemotherapy combined with targeted therapy and immunotherapy. At present, the patient has survived disease-free for 19 months without tumor recurrence, which is well beyond the median survival time for PSCCT (6-9 months) (7). This indicates that the treatment plan of surgery combined with immunotherapy benefits the patient. Overall, the survival rate of patients with PSCCT remains low even after aggressive surgical treatment and adjuvant chemotherapy, and immunotherapy and molecularly targeted therapy may be considered in the future.

In conclusion, PSCCT is an extremely aggressive malignant tumor that has a low incidence rate but a poor prognosis. Therefore, developing effective treatment strategies and raising survival rates require an early and precise diagnosis. Despite the limitations of US and CEUS in identifying the pathological type of thyroid cancer, the possibility of PSCCT should be considered based on the following ultrasonography characteristics: A large mass, a solid or mixed cystic-solid mass, presentation of hypoechoic or very hypoechoic echogenicity, irregular margins, microcalcifications observed internally, particularly extra-thyroidal extension, and CUES presenting with inhomogeneous hypo-enhancement and blurred borders. Additionally, CEUS demonstrates significant advantages in differentiating between benign and malignant thyroid nodules. Inhomogeneous hypo-enhancement is a reliable predictor of malignancy, whereas homogeneous hyper-enhancement, iso-enhancement or peripheral circumferential enhancement are more commonly observed in benign nodules.

US combined with CEUS should be extensively used in the early diagnosis of thyroid nodules. An early diagnosis will lead to better therapeutic prospects for the affected patients.

Acknowledgements

Not applicable.

Funding

No funding was received.

Availability of data and materials

The data generated in the present study are included in the figures and/or tables of this article.

Authors' contributions

CC, QX and LL were responsible for the conception and design of the manuscript. CC and QX drafted and wrote the manuscript. YD, JP and XH assisted in acquisition, analysis and revision of the associated figures. LL revised and proofread the manuscript. CC, QX, JP and LL confirm the authenticity of all the raw data. All authors have read and approved the final manuscript.

Ethics approval and consent to participate

The research was conducted ethically in conformity with the World Medical Association Declaration of Helsinki. Ethical approval for this case report was waived as the patient provided consent and the report contains nothing that may be considered a risk to patient privacy and integrity.

Patient consent for publication

Written informed consent was obtained from the patient for publication of this case presentation and any accompanying images.

Competing interests

The authors declare that they have no competing interests.

References

1. Yang S, Li C, Shi X, Ma B, Xu W, Jiang H, Liu W, Ji Q and Wang Y: Primary squamous cell carcinoma in the thyroid gland: A population-based analysis using the SEER database. World J Surg 43: 1249-1255, 2019.
2. LiVolsi VA and Merino MJ: Squamous cells in the human thyroid gland. Am J Surg Pathol 2: 133-140, 1978.
3. Sahoo M, Bal CS and Bhatnagar D: Primary squamous-cell carcinoma of the thyroid gland: New evidence in support of follicular epithelial cell origin. Diagn Cytopathol 27: 227-231, 2002.
4. Kebapci N, Efe B, Kabukcuoglu S, Akalin A and Kebapci M: Diffuse sclerosing variant of papillary thyroid carcinoma with primary squamous cell carcinoma. J Endocrinol Invest 25: 730-734, 2002.

5. Baloch ZW, Asa SL, Barletta JA, Ghossein RA, Juhlin CC, Jung CK, LiVolsi VA, Papotti MG, Sobrinho-Simões M, Tallini G and Mete O: Overview of the 2022 WHO classification of thyroid neoplasms. Endocr Pathol 33: 27-63, 2022.
6. Tessler FN, Middleton WD, Grant EG, Hoang JK, Berland LL, Teefey SA, Cronan JJ, Beland MD, Desser TS, Frates MC, *et al*: ACR thyroid imaging, reporting and data system (TI-RADS): white paper of the ACR TI-RADS committee. J Am Coll Radiol 14: 587-595, 2017.
7. Yan W, Chen H, Li J, Zhou R and Su J: Primary squamous cell carcinoma of thyroid gland: 11 case reports and a population-based study. World J Surg Oncol 20: 352, 2022.
8. Lam AK: Squamous cell carcinoma of thyroid: A unique type of cancer in World Health Organization Classification. Endocr Relat Cancer 27: R177-R192, 2020.
9. Zhang X, Chen L, Zhang H, Nong L and Wang F: Ultrasonic characterization of primary squamous cell carcinoma of the thyroid. J Ultrasound Med 41: 2317-2322, 2022.
10. Ou D, Ni C, Yao J, Lai M, Chen C, Zhang Y, Jiang T, Qian T, Wang L and Xu D: Clinical analysis of 13 cases of primary squamous-cell thyroid carcinoma. Front Oncol 12: 956289, 2022.
11. Ben Thayer M, Khanchel F, Helal I, Chiboub D, Raoueh H, Ben Brahim E, Jouini R and Chadli-Debbiche A: Epidemiological and histopathological characteristics of thyroid carcinoma in a Tunisian health care center. World J Otorhinolaryngol Head Neck Surg 10: 37-42, 2024.
12. Lugano R, Ramachandran M and Dimberg A: Tumor angiogenesis: Causes, consequences, challenges and opportunities. Cell Mol Life Sci 77: 1745-1770, 2020.
13. Zhan J and Ding H: Application of contrast-enhanced ultrasound for evaluation of thyroid nodules. Ultrasonography 37: 288-297, 2018.
14. Chen S, Peng Q, Zhang Q and Niu C: Contrast-enhanced ultrasound of primary squamous cell carcinoma of the thyroid: A case report. Front Endocrinol 11: 512, 2020.
15. Ma JJ, Ding H, Xu BH, Xu C, Song LJ, Huang BJ and Wang WP: Diagnostic performances of various gray-scale, color Doppler, and contrast-enhanced ultrasonography findings in predicting malignant thyroid nodules. Thyroid 24: 355-363, 2014.
16. Zhang X, Wei B, Nong L, Zhang H, Zhang J and Ye J: To diagnose primary and secondary squamous cell carcinoma of the thyroid with ultrasound malignancy risk stratification. Front Endocrinol 14: 1238775, 2023.
17. Haugen BR, Alexander EK, Bible KC, Doherty GM, Mandel SJ, Nikiforov YE, Pacini F, Randolph GW, Sawka AM, Schlumberger M, *et al*: 2015 American thyroid association management guidelines for adult patients with thyroid nodules and differentiated thyroid cancer: The American thyroid association guidelines task force on thyroid nodules and differentiated thyroid cancer. Thyroid 26: 1-133, 2016.
18. Liu G, Xu X, Chen G and Liu Z: Analysis of primary and secondary squamous cell carcinoma of the thyroid gland: A retrospective study. Gland Surg 10: 559-566, 2021.
19. Unadkat B, Phatak SV, Pavanan A and Patwa PA: Peripheral halo in a thyroid nodule-a sign of benignity. J Evol Med Dent Sci 10: 852-854, 2021.
20. Struller F, Senne M, Falch C, Kirschniak A, Konigsrainer A and Muller S: Primary squamous cell carcinoma of the thyroid: Case report and systematic review of the literature. Int J Surg Case Rep 37: 36-40, 2017.
21. Ordóñez NG: Value of thyroid transcription factor-1 immunostaining in tumor diagnosis: A review and update. Appl Immunohistochem Mol Morphol 20: 429-444, 2012.
22. Fassan M, Pennelli G, Pelizzo MR and Rugge M: Primary squamous cell carcinoma of the thyroid: Immunohistochemical profile and literature review. Tumori 93: 518-521, 2007.
23. Lam KY, Lo CY and Liu MC: Primary squamous cell carcinoma of the thyroid gland: An entity with aggressive clinical behaviour and distinctive cytokeratin expression profiles. Histopathology 39: 279-286, 2001.
24. Suzuki A, Hirokawa M, Takada N, Higuchi M, Yamao N, Kuma S, Daa T and Miyauchi A: Diagnostic significance of PAX8 in thyroid squamous cell carcinoma. Endocr J 62: 991-995, 2015.
25. Torrez M, Braunberger RC, Yilmaz E and Agarwal S: Primary squamous cell carcinoma of thyroid with a novel BRAF mutation and High PDL-1 expression: A case report with treatment implications and review of literature. Pathol Res Pract 216: 153146, 2020.
26. Xu B, Fuchs T, Dogan S, Landa I, Katabi N, Fagin JA, Tuttle RM, Sherman E, Gill AJ and Ghossein R: Dissecting anaplastic thyroid carcinoma: A comprehensive clinical, histologic, immunophenotypic, and molecular study of 360 cases. Thyroid 30: 1505-1517, 2020.
27. Ye M, Guo Z, Xu J, Jin Y, He X and Ge M: Primary squamous cell carcinoma of the thyroid has a molecular genetic profile distinct from that of anaplastic thyroid carcinoma: A whole exome sequencing and gene expression profiling study. Am J Surg Pathol 48: 1024-1031, 2024.
28. Ding W, Gao X and Ran X: Progress in diagnosing and treating thyroid squamous cell carcinoma under the 5th edition of WHO classification. Front Endocrinol 14: 1273472, 2023.
29. Limberg J, Ullmann TM, Stefanova D, Finnerty BM, Beninato T, Fahey TJ and Zarnegar R: Prognostic characteristics of primary squamous cell carcinoma of the thyroid: A national cancer database analysis. World J Surg 44: 348-355, 2020.
30. Au JK, Alonso J, Kuan EC, Arshi A and St John MA: Primary squamous cell carcinoma of the thyroid: A population-based analysis. Otolaryngol Head Neck Surg 157: 25-29, 2017.